Megalencephalic leukoencephalopathy with subcortical cysts type 1 (MLC1) due to a homozygous deep intronic splicing mutation (c.895-226T>G) abrogated in vitro using an antisense morpholino oligonucleotide

UNIVERSITÀ DEGLI STUDI DI TORINO

Megalencephalic Leukoencephalopathy with subcortical Cysts type 1 (MLC1) due to a homozygous deep intronic splicing mutation (c.895-226T>G) abrogated *in vitro* using an antisense morpholino oligonucleotide

Cecilia Mancini [1], Giovanna Vaula [2], Laura Scalzitti [1], Simona Cavalieri [1,3], Enrico Bertini [4], Chiara Aiello [4], Cinzia Lucchini [5], Richard A. Gatti [6], Alessandro Brussino [1*], Alfredo Brusco [1,3*].

[1] *Department of Genetics, Biology and Biochemistry, University of Torino, Italy*

[2] *Dept. Neuroscience, AOU. San Giovanni Battista, Torino, Italy*

[3] *S.C.d.U. Medical Genetics, A.O.U. San Giovanni Battista, Torino, Italy*

[4] *Laboratory of Molecular Medicine, Ospedale Pediatrico Bambino Gesù, Rome, Italy*

[5] *Unità Operativa Complessa di Neurologia, Ospedale di Ivrea, Italy*

[6] *Departments of Pathology and Laboratory Medicine, University of California, Los Angeles, David Geffen School of Medicine, Los Angeles, CA 90095-1732, USA*

*These authors contributed equally to the work

Corresponding author: Alfredo Brusco, *Department of Genetics, Biology and Biochemistry, University of Torino,* via Santena, 19 - 10126 Torino, Italy. Fax: +39 011 670 5668; *e-mail:* alfredo.brusco@unito.it

Keywords: MLC1, Megalencephalic leukoencephalopathy type 1, van der Knaap disease, homozygosis of a splicing mutation, antisense oligonucleotide, AMO

Running head: MLC1 deep intronic mutation

ABSTRACT

Megalencephalic leukoencephalopathy with subcortical cysts is an autosomal recessive disease characterized by early-onset macrocephaly, developmental delay, motor disability in the form of progressive spasticity and ataxia, seizures, cognitive decline and characteristic MRI findings. Mutations in two genes, *MLC1* (22q13.33; 75% of patients) or *HEPACAM* (11q24; 20% of patients) are associated with the disease.
We describe an adult MLC patient with moderate clinical symptoms. *MLC1* cDNA analysis from lymphoblasts showed a strong transcript reduction, and identified a 246-bp pseudoexon containing a premature stop codon between exons 10 and 11, due to a homozygous c.895-226T>G deep-intronic mutation. This category of mutations is often overlooked, being outside of canonically sequenced genomic regions. The mutation c.895-226T>G has a leaky effect on splicing leaving part of the full length transcript. Its role on splicing was confirmed using a minigene assay and an antisense morpholinated oligonucleotide (AMO) targeted to the aberrant splice site *in vitro*, which partially abrogated the mutation effect.

INTRODUCTION

Megalencephalic leukoencephalopathy with subcortical cysts is an autosomal recessive disease whose essential features include macrocephaly (large head) with onset in infancy, motor delay followed by motor disability in the form of progressive spasticity and ataxia, seizures, and cognitive decline. Neuroimaging shows extensive symmetric white-matter changes with subcortical cysts [1] . Despite severe neurological abnormalities, MLC has a milder clinical evolution compared to other infantile forms of leukodystrophies, e.g., those with peroxysomal or lysosomal defects [2].

Mutations in the *MLC1* gene on chromosome 22q13.33 are found in ~75% patients (megalencephalic leukoencephalopathy cysts type 1 or van der Knaap disease, OMIM#60404) [3]. In about 20% patients, the disease is explained by mutations in the hepatocyte cell adhesion molecule precursor gene (*HEPACAM*) on chromosome 11q24.2. *HEPACAM*-associated MLC can be inherited in an autosomal recessive form (classified as *MLC2A*, OMIM#613925) or in a less severe autosomal dominant form of "transient" MLC with or without mental retardation and/or autism (MLC2B, OMIM#613926) [4].

MLC1 is an oligomeric cytoplasmic membrane protein with eight predicted transmembrane segments. It is mainly localized in astrocyte-astrocyte junctions close to blood- and cerebrospinal fluid-brain barriers, Bergmann glia, and main axonal tracts [5]. Reported mutations interfere with MLC1 membrane localization [6]. A role in ion transport has been suggested due to its multi-pass membrane domains and the presence of an internal repeat similar to those found in ion channels [7]. Recently, it has been demonstrated that *MLC1* plays a role in anion channel activity, and its mutations reduce the regulatory volume of astrocytes, a key process in osmotic perturbation buffering in the central nervous system [8]. It remains to be elucidated whether MLC1 acts as a volume-regulated anion channel (VRAC) or contributes to the activation/regulation of a VRAC [8]. HEPACAM is an MLC1 interactor, predominantly expressed in the central nervous system, thus explaining why alterations in these two different proteins give rise to the same phenotype [6,9].

Here we describe a patient with MLC characterized by macrocephaly, juvenile-onset seizures and subcortical cysts, with moderate symptoms and slow progression. We identified the causative mutation in a homozygous deep-intronic variant in *MLC1* that introduces a pseudoexon with a premature stop codon and causes a leaky effect on splicing. The effect of the mutation on splicing was confirmed using a minigene assay and could be partially reverted *in vitro* with an antisense morpholinated oligonucleotide targeted to the aberrant splice site.

MATERIALS AND METHODS

Patients

The proband, clinically diagnosed with megalencephalic leukoencephalopathy with subcortical cysts, was from an Italian family (MLC-1-TO) with healthy relatives and 14 healthy siblings (Fig.1a). Peripheral blood was collected from 11 available family members (the mother and ten siblings), and a lymphoblastoid cell line (LCL) established from the MLC patient. Nine further cases were selected from a group of clinically and neuroradiologically defined MLC patients negative for mutations in known genes (E.B.). Informed consent was collected from all participants in the study.

DNA extraction and genetic analysis

Genomic DNA was extracted from peripheral blood (Qiagen, Hilden, Germany) following the manufacturer's instructions. Microsatellite markers at *MLC1* (chromosome 22q13.33) and *MLC2A* (chromosome 11q24.2) loci were chosen within a 1.5 Mb distance from the genes and amplified using KAPAFast polymerase under the conditions specified by the manufacturer (KAPA Biosystems, Woburn, MA, United States). Oligonucleotide sequences were: *355c18,* 5'-6FAM-gtgtcctgtgggtattccag and 5'-gaaccagggtgcagttcttg; D22S1169, 5'-6FAM-cacacacatgcacataatc and 5'-gaaccagggtgcagttcttg; chr11_124296, 5'-NED-cagctctaataagggcc and 5'-aagcctgcatgcctagagag; D11S4151, 5'-6FAM-gtcttcccaccttggatatgggta and 5'-aatgggcacctccaccctattagt. Amplification products were loaded into an ABI Prism 3100 Avant automated sequencer (Applied Biosystems, Foster City, CA, USA). Allele size was determined by comparison to a ROX-500 marker using the GeneScan software (Applied Biosystems). Haplotypes were manually reconstructed.

The 12 coding exons of the *MLC1* gene (RefSeq NM_015166.3) were PCR amplified using primer and conditions reported in Online Resources. Amplimers were purified using ExoSAP (MBI-Fermentas, Vilnius, Lithuania), and directly sequenced using the Big-Dye terminator cycle sequencing kit ver. 1.1 with an ABI Prism 3100 Avant automatic sequencer (Applied Biosystems).

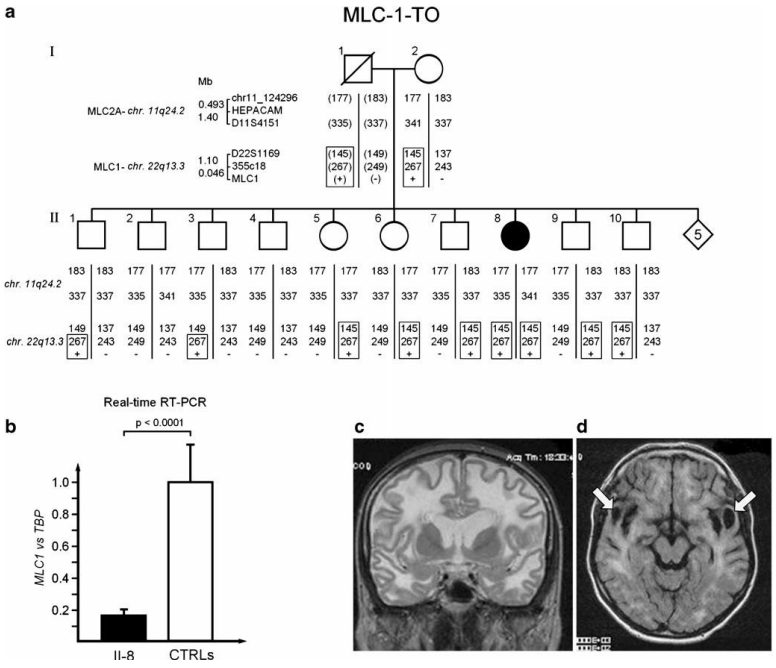

Fig. 1 Pedigree of the family MLC-1-TO, linkage and expression analyses. a Pedigree of the proband (II-8). Linkage analysis at MLC1 and HEPCAM loci with the reconstructed haplotypes is shown. Markers name, genes position, and the relative distances are reported. Genotypes in brackets (I-1) are deduced from segregation analysis. The symbol "+" indicates the presence of the c.895-226 T>G mutation. Boxed haplotypes are associated with the disease-causing mutation in MLC1. b LCLs expression analysis by real-time PCR of MLC1 versus TBP reference gene shows a strong reduction of the MLC1 transcript in patient II-8 compared with controls (19±2 %, dose ± SD). p Value is calculated following Student's t test. c MRI of the patient's brain at 48 years (T2-axial-weighted) and d (transverse flair). Diffuse hemispheric white matter abnormalities with preservation of internal capsule and ribbon-like aspect of hemispheric gray matter are visible in (c). Subcortical cysts in the anterior temporal regions are visible in (d) (arrows)

Expression analysis of MLC1

Total peripheral blood mononuclear cells (PBMC) were separated from blood using a Ficoll gradient. Total RNA was extracted using the RNeasy Plus Mini Kit (Qiagen), and retrotranscribed using the Transcriptor First Strand cDNA Synthesis kit (Roche Diagnostics, Mannheim, Germany). The expression levels of *MLC1* were measured in a duplex real-time PCR assay using primers 5'-agcagagtgtcccagcaagt (exon 9), 5'-agacgtgaggctgcttatgg (exon 10), the 6FAM labeled UPL#22 probe (Roche Diagnostics), and a commercial VIC-labeled TATA-binding protein TaqMan assay as a reference (Hs00427620_m1, Applied Biosystems). Reactions were carried out on an ABI 7500 Fast real-time PCR machine using the ABI TaqMan universal PCR master mix according to the manufacturer's instructions (Applied Biosystems). Efficiencies of the two assays were in the 90-110 % range. Each experiment was performed in triplicate with tree unrelated healthy controls. The mean Ct value was used for calculations, using the comparative delta-delta Ct method described by [10].

cDNA mutation analysis and c.895-226T>G mutation screening

The entire *MLC1* coding region was divided into four partially overlapping fragments ranging from 254 to 416 bp (Fig. 2a, regions A to D), gel analyzed and sequenced. The effect on cDNA splicing of the c.895-226T>G mutation was checked using the web applications Splice Site Prediction (http://www.fruitfly.org/seq_tools/splice.html) (Reese et al., 1997).

The mutation c.895-226T>G was confirmed in genomic DNA (gDNA) by direct sequencing after PCR-amplification with KAPA fast polymerase using the primers 10bF 5'-gtgctccgtggtcactctct and 10bR 5'-cgagtcggagccccagtaac at the annealing temperature of 60°C, under the conditions specified by the manufacturer (KAPA Biosystems).

A specific RT-PCR from ψ10b to exon 12 was performed using primers 11Fb: 5'-cagtggctcggtcacttttta and c12R: 5'- gctctccaggctttctcctt and the following conditions: 1 min at 95°C, followed by 14 cycles of 10 sec at 95°C, 10 sec at annealing temperature (56°C)+7°C-0.5°C/cycle and 10 sec at 72°C; then 25 cycles consisting of 10 sec at 95°C, 10 sec at annealing temperature 56°C and 10 sec at 72°C with KAPA fast polymerase (KAPA Biosystems).

The mutation c.895-226T>G in IVS10 introduces a *Msp*I restriction endonuclease site and was tested in controls using the *Msp*I restriction endonuclease (MBI-Fermentas, Vilnius, Lithuania): the gDNA amplimers of 200 healthy controls, obtained with primers 10bF+10bR and under conditions reported above were digested with *Msp*I endonuclease in the presence of the c.895-226G mutation the 496 bp amplimer is split into two bands (348 bp +121 bp).

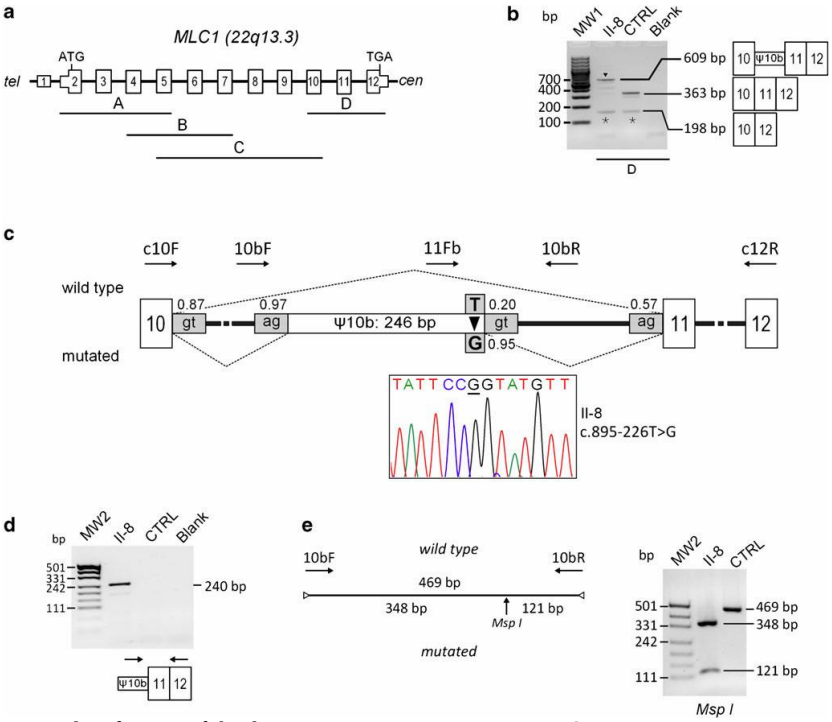

Fig. 2 Identification of the deep intronic mutation in patient II-8. a Schematic representation of the MLC1 gene structure (tel: telomere; cen: centromere; numbers indicate exons; larger boxes indicate coding region). MLC1 cDNAwas divided into four overlapping fragments (A–D). b cDNA amplification of fragment D, showing a major anomalous band of 609 bp (black arrowhead), whereas an unexpected band of 198 bp is present in both the patient and control (asterisks). This latter was characterized as an isoform lacking exon 11 (MLC1b). A scheme showing the structure of cDNA corresponding to each band is reported on the right. The 609 bp band contains part of intron 10 (pseudoexon, ψ10b). The pseudoexon results from a cryptic site activation downstream from the homozygous c.895-226 T>G mutation (c). Gene structure between exons 10 and 12 is shown in c: The relevant donor and acceptor splice sites and their strength are reported for the wildtype and muted sequences. Arrows indicate the primers used in the various experiments. The electropherogram showing the c.895-226 T>G homozygous mutation in the patient is also reported. d Using an RT-PCR with a primer internal to the pseudoexon and one in exon 12, a 240 bp band can be detected in patient II-8 but not in controls. e The c.895-226 T>G mutation introduces an MspI [CCGG] restriction endonuclease site that could be rapidly screened by a PCR/digestion. MW1: 100 bp ladder plus (MBI-Fermentas); MW2: pUC19/MspI

Minigene assay

A minigene assay was established to test the effects of the *MLC1* c.895-226T>G (IVS10) and the c.1059+16G>A (IVS11, rs#5771338) variants on splicing. Details are reported in Online Resources. Band quantification was performed with the ImageLAB software (Bio-Rad, Hercules, CA, USA) and statistical analyses with GraphPad Prism software (Graphpad Software, Lajolla, CA, USA).

Tissue expression analysis

We performed a semiquantitative real-time RT-PCR analysis amplifying fragment D (see Fig.2a) in cDNAs of adult human tissue (Human MTC Panel I, #636742 Clontech Laboratories, Mountain View, CA, USA) and fetal human tissue (Human Fetal MTC Panel, #636747 Clontech Laboratories) as templates using the primers and conditions specified in Online Resources.

Correction of MLC1 aberrant splicing by Antisense Morpholino Oligonucleotide (AMO)

The 25-mer AMO (ATCAGCTTGTGTTCAACATACCGGA, the mutation site is underlined) was designed to target the aberrant 3' splice site activated by the c.895-226T>G mutation in pre-mRNA. The AMO was synthesized and purified by Gene-Tools (LLC, Philomath, OR). Endo-Porter (Gene-Tools) was used to help lymphoblastoid cells incorporate the AMO. For AMO treatment, $5x10^5$ LCLs cells were resuspended in 0.5 ml 5% FBS/RPMI 1640 medium and AMO was added directly to the medium at the concentration indicated in figure 3 together with Endo-Porter (4 µl). Equal volumes of Endo-Porter were added to untreated cell cultures as controls. After 48 hours incubation, cells were collected and rinsed in PBS. Total RNA was extracted and cDNA retrotrascribed as described above. For RT PCR primers c10F and c12R were used to amplify both the full length and the mutant transcripts (see Online Resources).

RESULTS

Clinics and neuroradiology

The patient, a woman aged 49 yr., is the eighth of 15 siblings from healthy and reportedly unrelated parents. After an uneventful delivery, macrocephaly was noted during her first year of life, leading to an unspecific diagnosis of hydrocephalus (no radiological exams related to this diagnosis are available). A mild delay in psychomotor development was noticed and a very mild learning impairment was reported during schooling. At six years of age, several episodes of anxiety, sudden fear and claustrophobia occurred that were interpreted as epileptic seizures and treated with phenobarbital. At 22 yr. the patient presented her first tonic clonic seizures. The EEG documented bursts of sharp waves and a CT scan showed a diffuse supratentorial white matter hypodensity. At neurological examination, very mild cerebellar and pyramidal signs were noted.

At 27 yr. the patient acutely developed psychiatric symptoms (delusions and visual hallucinations) that required hospitalization and treatment with neuroleptic drugs. She gradually improved and five years later the neuroleptic and the antiepileptic treatments were discontinued without recurrence of both psychiatric symptoms and epileptic seizures.

The patient was stable until 44 yr. when she was hospitalized after an apparently accidental fall from a bicycle, with minor head trauma accompanied by loss of consciousness. At hospital admission, marked psychomotor agitation and motor impairment of right arm and leg were present, followed by prolonged coma. The patient remained unresponsive to verbal and nociceptive stimuli for few days. Once full consciousness recovered, she displayed a right hemiparesis with marked spasticity of the upper arm. Soon after the hospitalization a CT scan was performed that excluded post traumatic lesions and confirmed diffuse hypodensity of the supratentorial white matter. At MRI, a diffuse, symmetric signal abnormality involving frontal and parietal white matter and several subcortical cysts of the temporal lobes were present. The radiological picture prompted a diagnosis of MLC (Fig.1c-d).

Notably, soon after hospitalization, an increase in troponin levels together with evidence of septal and anterior hypokinesia at the transthoracic echocardiography suggested acute myocardial infarction. Cardiac enzymes and echocardiography normalized after two days, supporting a diagnosis of Tako-Tsubo syndrome [11].

Since then, the patient has undergone regular neurological follow up that documented a progressive worsening of her motor skills and four years after the acute event the patient was wheelchair bound. At the latest neurological examination, the patient presented truncal and gait ataxia, weakness and motor impairment of the right arm and of both legs, marked spasticity of right arm and leg, hypereflexia, bilateral Babinsky sign, intentional tremor of hands, dysarthric speech, and mild apraxia.

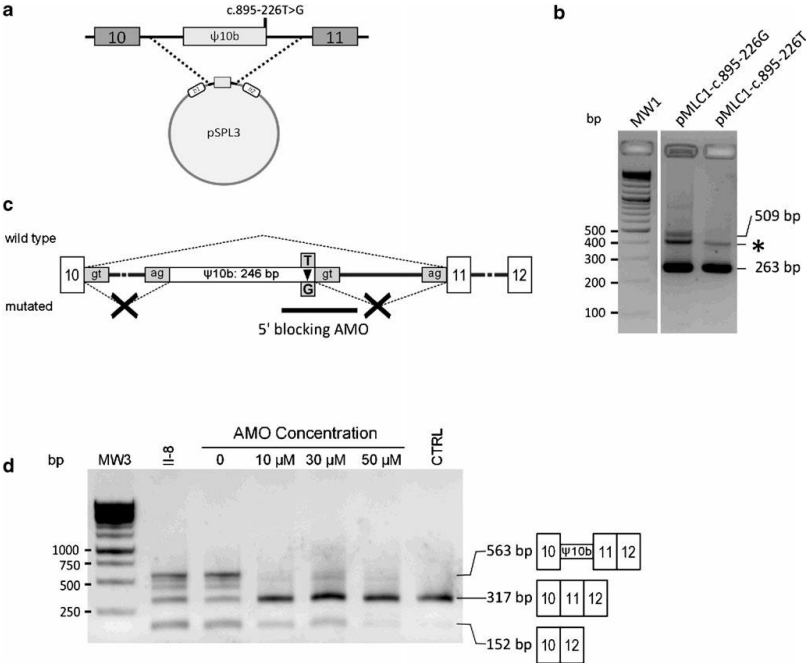

Fig. 3 Minigene assay and AMO strategy. The effect of c.895-226 T>G mutation on splicing was studied by a minigene assay (a). Part of MLC1 intron 10 was subcloned into a pSPL3 eukaryotic modified expression vector and transfected into HeLa cells. RT-PCR, using primers mapping into vector synthetic exons b1 and b2, displayed a 263 bp band corresponding to the spliced product between synthetic exons b1 and b2; an additional 509 bp band is present in the mutated clone only (pMLC1-c.895-226 G) and corresponds to an insertion of a 246 bp pseudoexon (b). The pseudoexon inclusion in the transcript occurs at a low efficiency, as seen by faint band intensity. Asterisk indicates an unexpected band (~400 bp), probably due to an internal splice site present in both the wild-type and mutated constructs. c–d Antisense morpholino oligonucleotide (AMO) strategy. Increasing amounts of AMO were transfected in patient's LCLs (II-8). The pseudoexon inclusion into MLC1 transcript was almost completely abrogated after AMO treatment. CTRL indicates a wild-type control. MW1, 100 bp ladder plus (MBI-Fermentas); MW3: DNA 1 kb ladder (MBI-Fermentas)

Genetic analyses

We exploited the availability of the genomic DNA from the mother and nine siblings of the patient for a linkage analysis to identify which of the two known *MLC* loci could be associated with the disease. Using microsatellite markers flanking the genes, *MLC2A* locus was excluded because the patient and one of her healthy brothers carried the same haplotypes at this locus (Figure 1a, II-2 and II-8). On the other hand, the

patient was homozygous for two markers close to the *MLC1* locus that are inherited from both parents, suggesting a possible consanguinity (Fig.1a). No sibling shared the same homozygous haplotype.
Considering *MLC1* as the possible disease-associated gene, we tested its involvement in the disease by measuring its expression in PBMCs. Real-time RT-PCR showed that *MLC1* mRNA was strongly reduced in our patient (≈17% ± 4% compared to controls, $p<0.0001$ Fig.1b). We sequenced the 12 *MLC1* coding exons, flanking intron boundaries, and part of the 5'- and 3'-UTR without finding any mutation. The minor alleles of two known SNPs in intron 4 (rs#79301) and intron 11 (rs#5771338) were found in homozygosis, further suggesting autozygosity/consanguinity.
MLC1 cDNA was amplified in four overlapping fragments (Fig. 2a). Fragment D showed the 363 bp normal band, and two unexpected bands: the shorter was present in both the patient and controls, and was found to be an alternative splicing isoform (see below) (Figure 2b, 198 bp); the larger was present in the patient only (Figure 2b, 609 bp). Sequencing showed that the 609 bp band corresponded to the insertion of one pseudoexon of 246 bp in intron 10 (named exon ψ10b), which contains in frame stop codons, probably causing a nonsense-mediated decay of the mRNA and thus explaining its reduced levels.
The cDNA and the genomic sequence surrounding the pseudoexon revealed a single possible causative mutation: a T>G homozygous change, c.895-226T>G (Fig. 2c). This change is not reported as a polymorphism in the dbSNP v.135. Calculating the splice site scores (i.e., strength of splicing) of the sequences adjacent to the 246 bp inclusion, the c.895-226T>G variant changes the splice site score from 0.20 in the wildtype to 0.95 in the mutant, creating a novel donor splice site and thereby resulting in the activation of a cryptic AG acceptor splice site 246 bp upstream (Fig. 2c). Using a specific primer within the pseudoexon (11Fb) and a reverse primer on exon 12 (c12R), we demonstrated the presence of a 240 bp band in the patient's cDNA only and not in ten normal controls (Fig. 2d). Finally, the c.895-226T>G change was not found in a group of 200 normal healthy controls from the same geographical region using restriction PCR digestion (see fig. 2e), further evidence that it was not a rare polymorphism. We also screened a group of nine clinically identified MLC patients, negative for mutations in both *MLC1* and *HEPACAM* genes, and did not find the c.895-226T>G, suggesting that it is a private mutation.

Minigene assay

Minigene constructs were obtained by cloning 469 bp of genomic DNA from IVS10, containing the pseudo exon ψ10b and flanking sequences, from patient II-8, and a healthy sibling (II-4) into the plasmid vector pSPL3 (Invitrogen) (Fig. 3a). Figure 3 shows the characteristic post-transfection spliced products of the two minigene constructs, as determined by direct PCR product sequencing. Both mutated and wild type clones show a strong band corresponding to the empty vector (Fig. 3b, 263 bp). However, the construct pMLC1-c.895-226G containing the mutation showed an additional larger segment containing the pseudoexon ψ10b (Fig. 3b, 509 bp). Both constructs also showed an unexpected band of approximately 400 bp, interpreted as nonspecific (Fig. 3b, asterisk).

Correction of MLC1 aberrant splicing by Antisense Morpholino Oligonucleotide (AMO)

We designed a specific AMO to mask the cryptic 5' splice site activated by the c.895-226T>G mutation and delivered them to the patient's lymphoblastoid cell line. Correction of splicing could already be observed at the lower dosage of 10 μM AMO, as demonstrated by RT-PCR, with the almost complete abrogation of the 246 bp pseudoexon (Fig. 3d). Increasing the AMO dose did not notably change the band pattern. We also noted a remarkable reduction of the *MLC1b* isoform (see below) in AMO treated cell lines.

MLC1 has an alternative isoform with exon 11 skipping

We further observed in the mRNA extracted from lymphoblasts of both the patient and healthy controls, the presence of an *MLC1* isoform lacking exon 11, subsequently named *MLC1b*. Because this variant is not reported in the genomic databases (see UCSC genome browser) we decided to investigate its expression pattern and its origin. We analyzed MLC1/MLC1b expression in several human tissue by RT-PCR using forward primer in exon 10 (c10F) and a reverse primer in exon 12 (c10R) and showed that the *MLC1b* isoform is ubiquitously expressed at low levels, with the exception of fetal brain, where the band corresponding to MLC1 and MLC1b isoforms have comparable intensity (Fig. 4a).

Performing the same test on lymphoblasts from healthy controls we noted the *MLC1b* isoform intensity was variable, and undetectable in some. Hypothesizing the presence of a genomic variant affecting splicing, we sequenced exon 11 and flanking introns, and noted that controls containing *MLC1b* were also carrying the minor allele "A" of rs#5771338, located at IVS11+16 position. This variant is a polymorphism with an allelic frequency of 12% in people of Northern and Western European ancestry (CEU population, http://www.1000genomes.org).

DISCUSSION

According to "The Human Gene Mutation Database" (http://www.hgmd.org/), ~10% of reported mutations in disease-associated genes are splicing mutations. Although most of them affect consensus sites, deep intronic mutations are increasingly being detected in human diseases: recent examples include HPRT deficiency, Usher syndrome type 2, Cystic Fibrosis, and Hemophilia A [12-15]. The importance of evaluating such splicing defects is well known, and has been underlined for MLC too [16].

Deep intronic mutations are easily overlooked, because they are not targeted by standard genetic screening and are missed even by more recent whole-exome sequencing methods. They are, however, particularly interesting from a therapeutic point of view. In case of a deep intronic mutation, the wild-type splice sites remain unchanged, and thus may be utilized to force the cell to skip the pseudoexon. Such achievement could be obtained using antisense oligonucleotides (AONs) that, targeting the donor, acceptor or branch site of the pre-mRNA, result in the skipping of the relative pseudoexon. The rescue of splicing defects has been demonstrated both *in vitro* and *in vivo*, and clinical trials are already in phase II for patients with Duchenne muscular dystrophy [17,18].

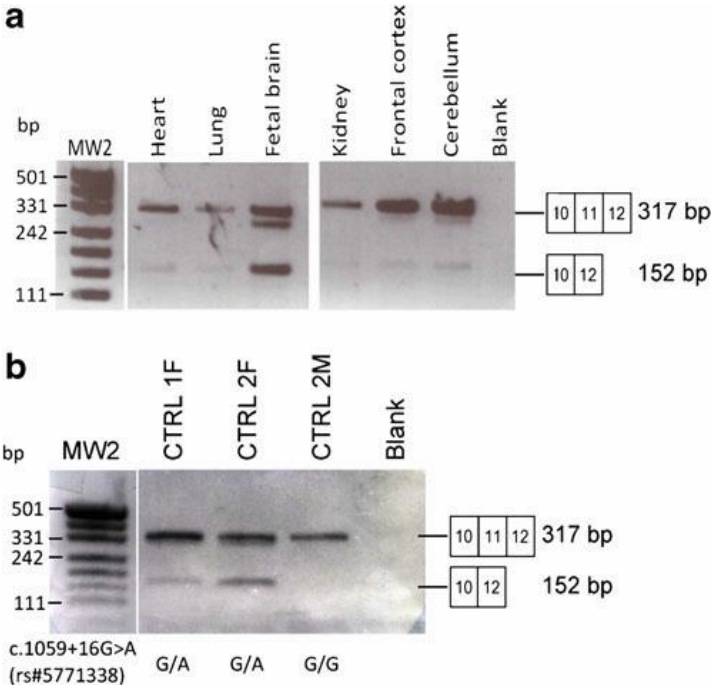

Fig. 4 MLC1b isoform with exon 11 skipping. a Using primers mapping in MLC1 exon 10 (c10F in Fig. 2c) and 12 (c12R in Fig. 2c), two amplification products of 317 and 152 bp were detected in human tissues. Sequencing revealed the former corresponding to exons 10–11–12, and the latter to exons 10–12. The second transcript variant, named MLC1b, is not reported in the genomic databases (e.g., genome.ucsc.org). The relative expression of the two transcripts is variable in different tissues; MLC1b is highly expressed in fetal brain. b RT-PCR analysis from three control LCLs showed that MLC1b is present only in carriers of the c.1059+16A variant at SNP rs#5771338

The diagnosis in this patient was initially puzzling. Clinical features overlapped with the MLC phenotype associated with *MLC1* mutations; however, macrocephaly, the first sign generally leading to diagnosis in the first years of life, was overlooked, together with a minor impairment and late onset (22 yr.) epileptic seizures which responded well to therapy. Only at 44 yr., an MRI exam, performed following head trauma, led to the diagnosis of MLC. Genetic confirmation was performed because the presence of only a single affected subject among 15 siblings was barely suggestive of an autosomal recessive disease.

Linkage analysis with microsatellite markers and expression analyses by real-time RT PCR on PBMCs proved that the disease was linked to the MLC1 locus. The absence of point mutations in the *MLC1* gene coding region prompted us to screen its cDNA. We found a deep intronic mutation in homozygosis (intron 10, c.895-226T>G), indicative of unreported consanguinity in the family. The c.895-226T>G change activates a donor splice site (Tgt > Ggt) that results in the inclusion of a 246 bp pseudoexon between exon 10 and 11. This mutation, not present in the dbSNP database, was also absent among 400 normal chromosomes, excluding that it might be a rare polymorphism. Further proof of its pathogenicity came from a minigene assay, which demonstrated inclusion of the pseudoexon only in the transcript from plasmids carrying the

mutation. The minigene construct yielded only a partial inclusion of the pseudoexon, suggesting a "leaky" mechanism of the mutation.

Our patient had a dramatic and irreversible deterioration after trauma, presenting an acute hemiparesis that required ruling out a post–traumatic lesion or an ictal event that, in turn, caused the fall from the bicycle. An acute deterioration caused by head trauma, although with gradual improvement, has been reported in MLC patients [19] and this also reminds of stress-related worsening seen in other leukoencephalopathies such as vanishing white matter disease and Leukoencephalopathy with brainstem and spinal cord involvement and lactate elevation [20-22]. The patient also presented a Tako-Tsubo syndrome, a transient left ventricular systolic dysfunction in the absence of obstructive coronary disease. Tako-Tsubo syndrome has been related to acute conditions leading to sympathetic dysregulation such as *status epilepticus* or subarachnoid haemorrhage. Few cases have been described in association to reversible posterior leukoencephalopathy, an acquired and transient white matter disorder, whose pathogenesis is still unclear [11].

Using an antisense morpholinated oligonucleotide (AMO, a stabilized antisense oligonucleotide variant) targeted to the cryptic donor splice site of the pseudoexon, we were able to restore *in vitro* normal splicing, even at the lowest doses, further proving that the c.895-226T>G variant was causing the pseudoexon activation .

Even if *MLC1* is a brain specific protein, our work shows that its transcript is easily detectable by RT-PCR in white blood cells, suggesting that patients testing negative for *MLC1* mutations (and probably also *HEPACAM*) should be screened for cDNA anomalies.

A variant transcript of *MLC1* without exon 11 (*MLC1b*), unreported in the databases, may also be related to the phenotype. We showed that *MLC1b* is present in a small percentage of transcripts in normal individuals (<5%) carrying the G>A SNP 16 bp downstream exon 11 (rs#5771338). In our patient, homozygous for the A variant, the splicing machinery, in the presence of c.895-226T>G mutation, may attempt a rescue of a functional MLC1 product, leading to an increase of the *MLC1b* isoform. This conclusion is also supported by the decrease *MLC1b* after AMO treatment. The role of the *MLC1b* isoform should be investigated in fetal brain, where it is highly expressed. We might speculate that *MLC1b* has a different function compared with *MLC1*, given its low expression in adult brain and the description of disease-associated splicing mutations possibly resulting in the skipping of exon 11, encoding for the transmembrane domain [23].

Three main conclusions are relevant from our work: 1. The identification of deep intronic mutations can solve clinical cases assigning the mutated gene to the disease; 2. Such mutations may shed light on new regulatory splicing elements, and 3. They may be used to study a therapeutic strategy based on antisense oligonucleotides. This having been said, each new AMO for each patient would also require pre-clinical trials for safety and efficacy, a major financial deterrent to personalized medicine that may need further consideration by regulatory agencies.

FIGURE LEGENDS

Figure 1 Pedigree of the family MLC-1-TO, linkage and expression analyses

(a) Pedigree of the proband (II-8). Linkage analysis at *MLC1* and *HEPCAM* loci with the reconstructed haplotypes is shown. Markers name, genes position and the relative distances are reported. Genotypes in brackets (I-1) are deduced from segregation analysis. The symbol "+" indicates the presence of the c.895-226T>G mutation. Boxed haplotypes are associated with the disease-causing mutation in *MLC1*.

(b) LCLs expression analysis by real-time PCR of *MLC1* versus *TBP* reference gene shows a strong reduction of the *MLC1* transcript in patient II-8 compared to controls (19±2%, dose ± S.D.). p-value is calculated following t-Student test. (c) MRI of the patient's brain at 48 yr. (T2 axial weighted) and (d) (transverse flair). Diffuse hemispheric white matter abnormalities with preservation of internal capsule and ribbon–like aspect of hemispheric gray matter are visible in (c). Subcortical cysts in the anterior temporal regions are visible in (d) (arrows).

Figure 2 Identification of the deep intronic mutation in patient II-8

(a) Schematic representation of the *MLC1* gene structure (tel: telomere; cen: centromere; numbers indicate exons; larger boxes indicate coding region). *MLC1* cDNA was divided into four overlapping fragments (A-D). (b) cDNA amplification of fragment D, showing a major anomalous band of 609 bp (black arrowhead), whereas an unexpected band of 198 bp is present in both the patient and control (asterisks). This latter was characterized as an isoform lacking exon 11 (*MLC1b*). A scheme showing the structure of cDNA corresponding to each band is reported on the right. The 609 bp band contains part of intron 10 (pseudoexon, ψ10b). The pseudoexon results from a cryptic site activation downstream from the homozygous c.895-226T>G mutation (c). Gene structure between exons 10-12 is shown in panel c: the relevant donor and acceptor splice sites and their strength are reported for the wild-type and muted sequences. Arrows indicate the primers used in the various experiments. The electropherogram showing the c.895-226T>G homozygous mutation in the patient is also reported. (d) Using an RT-PCR with a primer internal to the pseudoexon and one in exon 12, a 240 bp band can be detected in patient II-8 but not in controls. (e) The c.895-226T>G mutation introduces an *MspI* [CCGG] restriction endonuclease site that could be rapidly screened by a PCR/digestion. MW1: 100 bp ladder plus (MBI-Fermentas); MW2: pUC19/Msp*I* (MBI-Fermentas).

Figure 3 Minigene assay and AMO strategy

The effect of c.895-226T>G mutation on splicing was studied by a minigene assay (a). Part of *MLC1* intron 10 was subcloned into a pSPL3 eukaryotic modified expression vector and transfected into HeLa cells. RT-PCR, using primers mapping into vector synthetic exons b1 and b2, displayed a 263 bp band corresponding to the spliced product between synthetic exons b1 and b2; an additional 509 bp band is present in the mutated clone only (pMLC1-c.895-226G), and corresponds to an insertion of a 246 bp pseudoexon (b). The pseudoexon inclusion in the transcript occurs at a low efficiency, as seen by faint band intensity. Asterisk

indicates an unexpected band (~ 400 bp), probably due to an internal splice site present in both the wild-type and mutated constructs. (c-d) Antisense morpholino oligonucleotide (AMO) strategy. Increasing amounts of AMO were transfected in patient's LCLs (II-8). The pseudoexon inclusion into *MLC1* transcript was almost completely abrogated after AMO treatment. CTRL indicates a wild type control. MW1: 100 bp ladder plus (MBI-Fermentas); MW3: DNA 1Kb ladder (MBI-Fermentas).

Figure 4 *MLC1b* isoform with exon 11 skipping

(a) Using primers mapping in *MLC1* exon 10 (c10F in Fig.2c) and 12 (c12R in Fig.2c), two amplification products of 317 bp and 152 bp were detected in human tissues. Sequencing revealed the former corresponding to exons 10-11-12, and the latter to exons 10-12. The second transcript variant, named *MLC1b*, is not reported in the genomic databases (e.g., genome.ucsc.org). The relative expression of the two transcripts is variable in different tissues; *MLC1b* is highly expressed in fetal brain. (b) RT-PCR analysis from three control LCLs showed that *MLC1b* is present only in carriers of the c.1059+16A variant at SNP rs#5771338.

ACKNOWLEDGEMENTS

We thank Dr. D. Coviello for the pSPL3 vector (Invitrogen) and Prof. Nicola Migone for critical discussion. We are indebted to the patient and family members who collaborated in the study. This work was supported by Compagnia di San Paolo, Progetto finalizzato Neuroscienze entitled "Identification of a novel gene responsible for a form of adult-onset autosomal dominant leukodystrophy".

REFERENCES

1. van der Knaap MS, Barth PG, Stroink H, van Nieuwenhuizen O, Arts WF, Hoogenraad F, Valk J (1995) Leukoencephalopathy with swelling and a discrepantly mild clinical course in eight children. Ann Neurol 37 (3):324-334
2. Costello DJ, Eichler AF, Eichler FS (2009) Leukodystrophies: classification, diagnosis, and treatment. Neurologist 15 (6):319-328. doi:10.1097/NRL.0b013e3181b287c8
00127893-200911000-00004 [pii]
3. Leegwater PA, Boor PK, Yuan BQ, van der Steen J, Visser A, Konst AA, Oudejans CB, Schutgens RB, Pronk JC, van der Knaap MS (2002) Identification of novel mutations in MLC1 responsible for megalencephalic leukoencephalopathy with subcortical cysts. Hum Genet 110 (3):279-283
4. Lopez-Hernandez T, Ridder MC, Montolio M, Capdevila-Nortes X, Polder E, Sirisi S, Duarri A, Schulte U, Fakler B, Nunes V, Scheper GC, Martinez A, Estevez R, van der Knaap MS (2011) Mutant GlialCAM causes megalencephalic leukoencephalopathy with subcortical cysts, benign familial macrocephaly, and macrocephaly with retardation and autism. Am J Hum Genet 88 (4):422-432. doi:S0002-9297(11)00057-7 [pii]
10.1016/j.ajhg.2011.02.009
5. Teijido O, Casaroli-Marano R, Kharkovets T, Aguado F, Zorzano A, Palacin M, Soriano E, Martinez A, Estevez R (2007) Expression patterns of MLC1 protein in the central and peripheral nervous systems. Neurobiol Dis 26 (3):532-545. doi:S0969-9961(07)00031-9 [pii]
10.1016/j.nbd.2007.01.016
6. Lopez-Hernandez T, Sirisi S, Capdevila-Nortes X, Montolio M, Fernandez-Duenas V, Scheper GC, van der Knaap MS, Casquero P, Ciruela F, Ferrer I, Nunes V, Estevez R (2011) Molecular mechanisms of MLC1 and GLIALCAM mutations in megalencephalic leukoencephalopathy with subcortical cysts. Hum Mol Genet 20 (16):3266-3277. doi:ddr238 [pii]
10.1093/hmg/ddr238
7. Teijido O, Martinez A, Pusch M, Zorzano A, Soriano E, Del Rio JA, Palacin M, Estevez R (2004) Localization and functional analyses of the MLC1 protein involved in megalencephalic leukoencephalopathy with subcortical cysts. Hum Mol Genet 13 (21):2581-2594. doi:10.1093/hmg/ddh291
ddh291 [pii]
8. Ridder MC, Boor I, Lodder JC, Postma NL, Capdevila-Nortes X, Duarri A, Brussaard AB, Estevez R, Scheper GC, Mansvelder HD, van der Knaap MS (2011) Megalencephalic leucoencephalopathy with cysts: defect in chloride currents and cell volume regulation. Brain 134 (Pt 11):3342-3354. doi:awr255 [pii]
10.1093/brain/awr255
9. Favre-Kontula L, Rolland A, Bernasconi L, Karmirantzou M, Power C, Antonsson B, Boschert U (2008) GlialCAM, an immunoglobulin-like cell adhesion molecule is expressed in glial cells of the central nervous system. Glia 56 (6):633-645. doi:10.1002/glia.20640
10. Livak KJ, Schmittgen TD (2001) Analysis of relative gene expression data using real-time quantitative PCR and the 2(-Delta Delta C(T)) Method. Methods 25 (4):402-408
11. Akashi YJ, Nakazawa K, Sakakibara M, Miyake F, Koike H, Sasaka K (2003) The clinical features of takotsubo cardiomyopathy. QJM 96 (8):563-573
12. Corrigan A, Arenas M, Escuredo E, Fairbanks L, Marinaki A (2011) HPRT Deficiency: Identification of Twenty-Four Novel Variants Including an Unusual Deep Intronic Mutation. Nucleosides Nucleotides Nucleic Acids 30 (12):1260-1265. doi:10.1080/15257770.2011.590172
13. Vache C, Besnard T, le Berre P, Garcia-Garcia G, Baux D, Larrieu L, Abadie C, Blanchet C, Bolz HJ, Millan J, Hamel C, Malcolm S, Claustres M, Roux AF (2011) Usher syndrome type 2 caused by activation of an USH2A pseudoexon: Implications for diagnosis and therapy. Hum Mutat. doi:10.1002/humu.21634
14. Costa C, Pruliere-Escabasse V, de Becdelievre A, Gameiro C, Golmard L, Guittard C, Bassinet L, Bienvenu T, Georges MD, Epaud R, Bieth E, Giurgea I, Aissat A, Hinzpeter A, Costes B, Fanen P, Goossens M, Claustres M, Coste A, Girodon E (2011) A recurrent deep-intronic splicing CF mutation emphasizes the importance of mRNA studies in clinical practice. J Cyst Fibros 10 (6):479-482. doi:S1569-1993(11)00120-2 [pii]
10.1016/j.jcf.2011.06.011
15. Castaman G, Giacomelli SH, Mancuso ME, D'Andrea G, Santacroce R, Sanna S, Santagostino E, Mannucci PM, Goodeve A, Rodeghiero F (2011) Deep intronic variations may cause mild hemophilia A. J Thromb Haemost 9 (8):1541-1548. doi:10.1111/j.1538-7836.2011.04408.x

16. Ilja Boor PK, de Groot K, Mejaski-Bosnjak V, Brenner C, van der Knaap MS, Scheper GC, Pronk JC (2006) Megalencephalic leukoencephalopathy with subcortical cysts: an update and extended mutation analysis of MLC1. Hum Mutat 27 (6):505-512. doi:10.1002/humu.20332
17. Aartsma-Rus A, den Dunnen JT, van Ommen GJ (2010) New insights in gene-derived therapy: the example of Duchenne muscular dystrophy. Ann N Y Acad Sci 1214:199-212. doi:10.1111/j.1749-6632.2010.05836.x
18. Lu QL, Yokota T, Takeda S, Garcia L, Muntoni F, Partridge T (2011) The status of exon skipping as a therapeutic approach to duchenne muscular dystrophy. Mol Ther 19 (1):9-15. doi:mt2010219 [pii] 10.1038/mt.2010.219
19. Bugiani M, Moroni I, Bizzi A, Nardocci N, Bettecken T, Gartner J, Uziel G (2003) Consciousness disturbances in megalencephalic leukoencephalopathy with subcortical cysts. Neuropediatrics 34 (4):211-214. doi:10.1055/s-2003-42209
20. Serkov SV, Pronin IN, Bykova OV, Maslova OI, Arutyunov NV, Muravina TI, Kornienko VN, Fadeeva LM, Marks H, Bonnemann C, Schiffmann R, van der Knaap MS (2004) Five patients with a recently described novel leukoencephalopathy with brainstem and spinal cord involvement and elevated lactate. Neuropediatrics 35 (1):1-5
21. Kaczorowska M, Kuczynski D, Jurkiewicz E, Scheper GC, van der Knaap MS, Jozwiak S (2006) Acute fright induces onset of symptoms in vanishing white matter disease-case report. Eur J Paediatr Neurol 10 (4):192-193
22. Vermeulen G, Seidl R, Mercimek-Mahmutoglu S, Rotteveel JJ, Scheper GC, van der Knaap MS (2005) Fright is a provoking factor in vanishing white matter disease. Ann Neurol 57 (4):560-563
23. Leegwater PA, Yuan BQ, van der Steen J, Mulders J, Konst AA, Boor PK, Mejaski-Bosnjak V, van der Maarel SM, Frants RR, Oudejans CB, Schutgens RB, Pronk JC, van der Knaap MS (2001) Mutations of MLC1 (KIAA0027), encoding a putative membrane protein, cause megalencephalic leukoencephalopathy with subcortical cysts. Am J Hum Genet 68 (4):831-838